Published in final edited form as:

Cell. 2015 April 23; 161(3): 501–512. doi:10.1016/j.cell.2015.03.040.

Substrates Control Multimerization and Activation of the Multi-domain ATPase Motor of Type VII Secretion

Oren S. Rosenberg[1,*], **Dustin Dovala**[2,*], **Xueming Li**[3], **Lynn Connolly**[1,5], **Anastasia Bendebury**[2], **Janet Finer-Moore**[4], **James Holton**[4,6], **Yifan Cheng**[4], **Robert M. Stroud**[4], and **Jeffery S. Cox**[2]

[1]Department of Medicine, Division of Infectious Diseases, UCSF Medical Center, University of California, San Francisco, CA 94143-0654, USA

[2]Department of Microbiology and Immunology, Program in Microbial Pathogenesis and Host Defense, University of California, San Francisco, CA 94158, USA

[3]School of Life Sciences, Tsinghua University, Beijing, China, 100084

[4]Department of Biophysics and Biochemistry, University of California, San Francisco, CA 94158, USA

[5]Achaogen, Inc. South San Francisco, CA 94080, USA

[6]Lawrence Berkeley National Laboratory, MS6-2100, Berkeley, CA 94720, USA

Summary

Mycobacterium tuberculosis and *Staphylococcus aureus* secrete virulence factors via Type VII protein secretion (T7S), a system that intriguingly requires all of its secretion substrates for activity. To gain insights into T7S function, we used structural approaches to guide studies of the putative translocase EccC, a unique enzyme with three ATPase domains, and its secretion substrate EsxB. The crystal structure of EccC revealed that the ATPase domains are joined by linker/pocket interactions that modulate its enzymatic activity. EsxB binds via its signal sequence to an empty pocket on the C-terminal ATPase domain, which is accompanied by an increase in ATPase activity. Surprisingly, substrate binding does not activate EccC allosterically, but rather by stimulating its multimerization. Thus, the EsxB substrate is also an integral T7S component, illuminating a mechanism that helps explain interdependence of substrates and suggests a model in which binding of substrates modulates their coordinate release from the bacterium.

Correspondence to: jeffery.cox@ucsf.edu; Phone: (415) 502-4240; Fax: (415) 502-4315.

*These two authors contributed equally to this work

Author Contributions

O.S.R. and D.D. contributed equally to this work. O.S.R and J.S.C. conceived the research; O.S.R., D.D., X.L., Y.C., R.M.S., and J.S.C., designed experiments; O.S.R., D.D., X.L., L.C., and A.B. collected data; O.S.R., D.D., X.L., J.H., J.F.M., Y.C., R.M.S., and J.S.C. analyzed data; O.S.R., D.D., and J.S.C wrote the manuscript. All authors commented on the scientific content of the manuscript.

Introduction

While all cells secrete proteins through the conserved Sec system, bacteria also utilize specialized secretion systems to interact with their environment (Waksman, 2012). These systems are particularly important for bacterial pathogens, as they allow for regulated secretion of virulence factors into eukaryotic cells during infection. The Type VII secretion (T7S) system, the only specialized secretion system found exclusively in Gram-positive bacteria (Huppert et al., 2014; Waksman, 2012), is required for virulence of several bacterial pathogens, including *Mycobacterium tuberculosis* (Guinn et al., 2004; Houben et al., 2014; Hsu et al., 2003; Stanley et al., 2003), *Mycobacterium marinum* (Davis and Ramakrishnan, 2009; Gao et al., 2004), and *Staphylococcus aureus* (Burts et al., 2005). The significance of this secretion system is further highlighted by the fact that loss of the ESX-1 T7S system in *M. tuberculosis* is the most important genetic difference between virulent strains that cause tuberculosis and the live attenuated vaccine strain, BCG (Brodin et al., 2006; Mahairas et al., 1996; Pym et al., 2003). However, despite its medical importance and its broad evolutionary conservation, the molecular architecture, mechanism of secretion, and regulation of T7S are unknown.

T7S systems have been identified in many Gram-positive organisms and are defined by the presence of two conserved elements: EccC, a membrane-bound protein with three predicted ATPase domains, and EsxB, a small secretion substrate containing a WXG motif (Bitter et al., 2009; Pallen, 2002). Other components have been genetically linked to T7S, but these are not universally conserved (Abdallah et al., 2007). EccC and EsxB interact physically (Stanley et al., 2003) and the last seven amino acids of EsxB constitute a “signal-sequence” that is necessary and sufficient for secretion through the ESX-1 system (Champion et al., 2006), although additional signals adjacent to these sequences are also required for full secretion (Daleke et al., 2012; Sysoeva et al., 2014). The molecular basis of T7S substrate-targeting selection is not known, and our understanding of substrate recognition has been mostly limited to yeast two-hybrid and genetic studies. One interesting feature of T7S is that substrates are co-dependent for secretion (Fortune et al., 2005), in that genetic removal of one substrate abrogates secretion of all other substrates through a specific T7S system. This unique feature of T7S has complicated the study of individual virulence factors in the context of infection and has thwarted attempts to genetically engineer these systems to secrete heterologous proteins.

EccC has a unique multi-domain structure consisting of a two-pass transmembrane domain, a short domain of unknown function (DUF) and three P-loop NTPase domains that share approximately 20% identity to one another (Figure 1A). The ATPase domains are evolutionarily related to the ASCE (**A**dditional **S**trand **C**onserved **G**lutamate) fold family that includes protein and DNA directed mechanoenzymes such as FtsK, VirD4 (TrwB) and VirB4 (TrwK) (Erzberger and Berger, 2006). These motor proteins generally assemble into hexameric rings with the ATPase activity dependent on “arginine finger” residues that extend into adjacent monomers to form the active site (Ahmadian et al., 1997). The individual ATPase domains of EccC are unique in that each has a long N-terminal linker that is of unknown function but contains several motifs that are highly conserved among all of the EccC proteins.

We present here a series of structures of EccC, both with and without the EsxB signal sequence, which reveal that EccC exists in an autoinhibited state as a tightly integrated set of three ATPase domains joined to one another through specific linker/pocket interactions. We show that EccC activity is activated by disruption of one of these linker interactions and further activated through substrate-mediated multimerization of the enzyme. Our findings suggest that substrates, in addition to serving roles outside of the cell, are also necessary components of the secretion apparatus itself, and provide a mechanistic explanation for the unique interdependence of substrate secretion in T7S.

Results

The EsxB Signal Sequence Binds the EccC Translocase but does not Activate its ATPase Activity

To understand the nature of the interaction between EccC and EsxB using an *in vitro* system, we screened a panel of EccC/EsxB pairs from various bacterial species and found robust expression in *E. coli* of the cytoplasmic portion of EccC from the thermophilic actinobacterium *Thermomonospora curvata* (*Tc*EccC$_{(cyto)}$) and its cognate EsxB partner (*Tc*EsxB). The *T. curvata* secretion system shares close homology with other actinomycete T7S systems and contains all of the conserved components identified in the *M. tuberculosis* Esx system including EsxA, EsxB, EccC, EccD, EccB, and MycP1 (Bitter et al., 2009) (Figure S1A). *Tc*EccC$_{(cyto)}$, *Tc*EsxA and *Tc*EsxB were all stable in isolation and strongly bound one another to form an EccC:EsxB:EsxA complex (Figure 1B; Figure S1B and S1C). Similar to yeast two-hybrid studies with *M. tuberculosis* proteins (Champion et al., 2006), the last seven amino acids of *Tc*EsxB specifically targeted the substrate to *Tc*EccC, and swapping this sequence with the C-terminus of *Mt*EsxB$_1$ completely reversed the specificity (Figure 1C). Thus the known EccC interactions of the virulence associated ESX-1 system of *M. tuberculosis* are recapitulated in our model system.

In the ESX-1 system in *M. tuberculosis*, *Mt*EccC is split into two polypeptides, *Mt*EccCa (containing the trans- and juxtamembrane regions and ATPase$_1$) and *Mt*EccCb (containing ATPase$_2$ and ATPase$_3$), which interact with one another to form a complete *Mt*EccCab complex (Stanley et al., 2003). The substrate *Mt*EsxB interacts exclusively with *Mt*EccCb and not with *Mt*EccCa and we found this feature was conserved in our *T. curvata* system. When we artificially split *Tc*EccC into "*Tc*EccCa" and "*Tc*EccCb" fragments orthologous to the tuberculosis ESX-1 proteins, these fragments interacted robustly in the two-hybrid assay (Figure S1B). Likewise, EsxB interacted directly with *Tc*EccCb but not *Tc*EccCa, which parallels the ESX-1 system (Figure S1B and S1D).

In analogy with other phylogenetically related translocases (Guglielmini et al., 2013), which are often strongly activated by their substrates (Massey et al., 2006), we hypothesized that binding of *Tc*EccC$_{(cyto)}$ to the substrate *Tc*EsxB would activate its ATPase domains. However we could not measure any ATPase activity in the *Tc*EccC$_{(cyto)}$ or *Tc*EccCb proteins, either in the presence or absence of *Tc*EsxB (Figure S1E). Likewise, the nucleotide binding state of EccC had no effect on the apparent K_D of signal sequence binding (Figure S1F). This unexpected result suggested that the binding to EccC does not immediately lead to work being done on the substrate.

The Structure of *Tc*EccCb Bound to the Signal Sequence

In order to understand the interaction between EsxB and EccC, we solved the structure of *Tc*EccCb (containing $ATPase_2$ and $ATPase_3$) using data to 3.24 Å resolution, in combination with a peptide containing the last 23 residues of the *Tc*EsxB substrate, including the C-terminal signal sequence (Figure 2A; Figure S2A and Table S2). Both $ATPase_2$ and $ATPase_3$ are clearly bound to ATP in the structure (Figure 2B and 2C) suggesting that the ATPase activity of these domains is indeed extremely low, even in the presence of saturating amounts of EsxB signal sequence peptide. This ATPase-inactivated state appears to be evolutionarily conserved, as a high-resolution crystal structure of a fragment of the related EssC ATPase from *Geobacillus thermodenitrificans* ("*Gb*EssCb") has a very similar structure, with both domains bound to ATP (Figure S2B).

The C-terminus of the signal sequence peptide, which was previously thought to be unstructured (Renshaw et al., 2005), forms a short amphipathic helix (residues 96–103) that interacts exclusively with the hydrophobic pocket on $ATPase_3$ ($pocket_3$) (Figure 2A). This C-terminal helix is likely a common feature of all EsxB homologs (Poulsen et al., 2014). The helix was also present in a higher resolution structure of the full length *Tc*EsxBA complex in the absence of $ATPase_3$ (Figure 2D and Table S2). Here, we observed the characteristic helical hairpin seen in all EsxB homolog proteins, however in our structure the chain makes a turn through a short extended region (residues 93–95) before ending in a helix that matches the length of helix observed in the ATPase complex structure. Of note, this helix is found in a crystal contact with an adjacent symmetry related molecule, which could artificially stabilize the helical structure. Although present in the EsxB fragment crystallized with EccC, the Y-X-X-X-D/E motif implicated in secretion (Daleke et al., 2012; Sysoeva et al., 2014) was disordered in our crystal, suggesting that it is not involved in recognition of the signal sequence motif. Importantly, $pocket_3$ is distant from the ATP catalytic site and binding of the peptide does not appear to alter the ATP binding ability of $ATPase_3$. Mutation of any of the EsxB interaction residues on either EsxB or EccC completely abrogated the interaction, demonstrating the specificity of its binding to $pocket_3$ (Figure 2E and S2C). Together, these data show that *Tc*EsxB is targeted to *Tc*EccCb through specific binding to the hydrophobic $pocket_3$ on $ATPase_3$, but binding of the C-terminus of *Tc*EsxB neither requires nor enhances nucleotide hydrolysis or exchange.

Because EccC lacked ATPase activity with or without substrate, we examined the evolutionary conservation of each ATPase domain amongst many unique EccC orthologs to determine if the residues required for ATPase activity are conserved. We found that the catalytic residues of $ATPase_2$ and $ATPase_3$ are highly degenerate with respect to other related ATPases, especially in the catalytic glutamate of the Walker B motif (Figure S2D). Such changes might be expected to greatly reduce or eliminate ATP hydrolysis (Wendler et al., 2012), which is consistent with the presence of ATP in these domains observed in our crystal structures. In contrast, $ATPase_1$ is highly conserved with its closest known homolog, the motor protein FtsK, suggesting $ATPase_1$ may serve as the active motor domain for EccC. Thus, $ATPase_2$ and $ATPase_3$ appear to be naturally suboptimal ATPases, similar to the catalytically inactive domains of other multimeric ATPases such as dynein (Carter et al., 2011) and the F_1-ATPase (Walker, 2013).

ATPase$_1$ is Inhibited by its Interaction with ATPase$_2$

To understand the structure of ATPase$_1$ and its relationship to ATPase$_2$ and ATPase$_3$, we solved the crystal structure of the full cytoplasmic domain of *Tc*EccC, "*Tc*EccC$_{(cyto)}$," using data to 2.9 Å resolution (Figure 3A; Figure S3A and S3B; Table S3). Although the full protein is present in the crystal (Figure S3C), the N-terminal "DUF" domain and linker$_1$ are disordered in the structure and could not be modeled. The structure is monomeric, as it is in solution (Figure S3D), and ATPase$_2$ and ATPase$_3$ are very similar in both their conformation and nucleotide binding state compared to the *Tc*EccCb structure (RMSD 0.7 Å), showing that binding of the signal sequence does not alter EccC's structure in these domains. The interface between ATPase$_1$ and ATPase$_2$ is remarkably similar to the interface between ATPase$_2$ and ATPase$_3$, joining together the three domains in a direct translation where the only interfaces between the domains are mediated by the inter-domain linkers. Highlighting the general importance of these linker interactions, removal of the N-terminal 34 amino acids homologous to linker$_2$ on *Mt*EccCb completely blocked binding to *Mt*EccCa (Figure S3E and S3F). Single-particle electron microscopy and 3D reconstruction of *Tc*EccC$_{(cyto)}$ and a related ATPase from *Geobacillus thermodenitrificans* revealed a similar monomeric structure that was remarkably rigid, as illustrated in the homogeneity of the class averages (Figure 3B and 3C; Figure S3G, S3H, S3I, and S3J). The DUF domain, which is required for secretion *in vivo* (Figure S3K), is also visible in these images, though its density is reduced, likely due to averaging of multiple flexible states.

In ATPase$_1$ the nucleotide binding residues and nucleotide loading is strikingly different from the other two domains (Figure 3D and 3E). Despite the high ATP concentration in the crystallization solution (5 mM), ATPase$_1$ contains a sulfate ion in the active site (Figure 3A) whereas ATPase$_2$ and ATPase$_3$ are bound to ATP as they were in the signal sequence-bound structure (Figure 2). Several structural features of the ATPase$_1$ catalytic site are strongly reminiscent of the ATP "empty" (β_E) subunit of the F_1-ATPase (Figure 3D and 3E) which is known to have a very low affinity for nucleotide (Menz et al., 2001; Senior, 2012). In particular, the Walker A lysine is rotated into an unfavorable rotamer and bound to the Walker B aspartate, displacing the binding of magnesium in the active site and likely preventing binding of ATP. An analysis of all P-loop ATPases in the Protein Data Bank (Berman et al., 2002) that contain both ATP-bound and ATP-unbound subunits in the asymmetric unit found that this configuration of the enzymatic residues in the ATP binding site is very unusual under these conditions and is essentially restricted to structural models of the empty state of the F1-ATPase (Figure 3F and 3G).

Despite the low affinity state in the crystal, the ability of ATPase$_1$ to bind ATP is required *in vivo* (Figure 3H and Figure S3L, S3M, and S3N) showing that cycling of ATPase$_1$ into an ATP avid conformation is required for the function of the secretion system. We conclude that we have captured a low-nucleotide-affinity state of ATPase$_1$ that must be reversed during the EccC catalytic cycle.

Overlaying the three ATPase domains revealed that the linker-pocket interactions of ATPase$_1$ and ATPase$_2$ are analogous to signal sequence binding of ATPase$_3$ (Figure 4A). In particular, the important residues for signal sequence binding in pocket$_3$ have clear

homologs in the linker$_2$-pocket$_1$ interaction (Figure 4B). Since ATPases are often modulated by the effect of N- and C-terminal appendages (Besprozvannaya et al., 2013; Karamanou et al., 1999; Peña et al., 2011), we hypothesized that the attachment between pocket$_1$ and linker$_2$ might allosterically regulate ATPase$_1$, locking it into the low affinity form seen in the crystal structure and leading to the low catalytic rate we observed *in vitro*. Much of the interface between ATPase$_1$ and linker$_2$ is mediated by a 100% conserved arginine in pocket$_1$, R543, that interacts with W762 and L763 in linker$_2$ (Figure 5A and 5B). We reasoned that loss of this interaction might mimic an allosteric effector binding in pocket$_1$ in a manner analogous to signal sequence binding to ATPase$_3$ and modulate the activity of ATPase$_1$. Indeed, mutation of R543 to alanine resulted in a sharp increase in EccC ATPase activity (Figure 5C). Additional mutation of an ATPase$_1$ catalytic residue (E593Q) completely inhibited this activation, suggesting that this increase in ATPase activity is dependent on the activity of ATPase$_1$. Because R543 does not make any direct interactions with the ATP binding or catalytic residues, these results strongly suggest that the activity of ATPase$_1$ is modulated allosterically by its interaction with the linker. Mutation of the equivalent residue at the ATPase$_2$-ATPase$_3$ interface had no significant effect on the activity of the enzyme. Therefore, we conclude that the activity of ATPase$_1$ is controlled through its pocket-linker interaction with ATPase$_2$. Importantly, mutation of R543 to alanine in *Mt*EccCa$_1$ severely reduced secretion of EsxB by *M. tuberculosis* (Figure S4A and S4B), indicating that the interface between ATPase$_1$ and ATPase$_2$ is critical for the secretion process. This is consistent with a model in which this interface couples substrate recognition in EccCb (ATPase$_2$ and ATPase$_3$) with EccCa (ATPase$_1$) activity.

EccC ATPase Activation by Substrate Binding

In contrast to the wild-type enzyme, addition of *Tc*EsxB to the *Tc*EccC$_{(cyto,R543A)}$ activated mutant led to a five-fold, saturating increase in the ATPase activity (Figure 6A) revealing that substrates can contribute to EccC activation if the autoinhibitory interaction between ATPase$_1$ and ATPase$_2$ is removed. Mutation of *Tc*EsxB residues responsible for the interaction with ATPase$_3$ abrogated stimulation, demonstrating that the effect is specific to signal sequence binding (Figure S4C). However, mutation of the mutation of the catalytic residues in ATPase$_2$ and ATPase$_3$ significantly reduced, but did not eliminate, overall ATPase activity (Figure S4E). In accord with this finding, ATP binding by ATPase$_2$ and ATPase$_3$ is also required for secretion *in vivo* (Figure 3H). In contrast, ATPase$_2$ and ATPase$_3$ alone had no activity and were not stimulated by *Tc*EsxB (Figure 6A). Thus, although binding of ATP by ATPase$_2$ and ATPase$_3$ is required for full activity of EccC, these domains act to regulate the activity of ATPase$_1$ rather than additively contribute to overall ATPase activity. This is consistent with recent genetic evidence that the different ATPase domains play distinct roles during secretion *in vivo* (Ramsdell et al., 2014).

EccC Activity is Controlled by Multimerization

Binding of the EsxB signal sequence to ATPase$_3$ appears to be a simple molecular recognition event (Figure 2), and our results suggest that binding is unlikely to change the conformation of ATPase$_1$. We thus reasoned that substrate binding could activate EccC via regulating multimerization. Indeed, the related FtsK and TrwB ATPases form multimers during their catalytic cycle in which arginine residues (“R-fingers”) complete the active site

of neighboring subunits (Gomis-Rüth et al., 2001; Massey et al., 2006; Wendler et al., 2012). $ATPase_1$ has a completely conserved R- finger (Figure S4G and S4H) that is required for secretion *in vivo* (Figure S4I), implying that formation of the active site of $ATPase_1$ also involves multimerization. Furthermore, expression of ATPase-deficient versions of EccC in wild-type bacteria has a dominant- negative effect on secretion, consistent with this notion (Ramsdell et al., 2014).

In order to investigate the role of multimerization in the activation of EccC we measured the dependence of k_{cat} on increasing concentrations of enzyme. In the absence of multimerization, the k_{cat} should be a constant property of the enzyme, but if the catalytic pocket of one ATPase molecule is assembled *in trans* with an arginine donated by a different ATPase molecule, the k_{cat} of the enzyme should increase as more arginine fingers become available with increasing concentration of enzyme. In the absence of *Tc*EsxB, neither *Tc*$EccC_{(cyto)}$ nor *Tc*$EccC_{(cyto,R543A)}$ exhibited concentration- dependent ATPase activation (Figure 6B) suggesting their activity was not dependent on multimeriziation. In contrast, in the presence of a 10-fold excess of *Tc*EsxB (*Tc*EsxB+*Tc*$EccC_{(cyto,R543A)}$), the ATPase activity was strongly concentration dependent. To guarantee a one-to-one molar ratio between *Tc*EsxB and *Tc*EccC, we fused *Tc*EsxB via a flexible 14 amino acid linker to the C-terminus of *Tc*$EccC_{(cyto,R543A)}$. This protein was dimeric as determined by analytical ultracentrifugation (Figure S4F), and similarly to the *Tc*EsxB+*Tc*$EccC_{(cyto,R543A)}$ complex the k_{cat} of this chimera was highly concentration dependent (Figure 6B), with a maximal activity similar to the saturated *Tc*EsxB:*Tc*$EccC_{(cyto,R543A)}$ complex (>100-fold over wild-type). Mutation of the R-finger residue in the activated, substrate-ATPase fusion protein (*Tc*EsxB- *Tc*$EccC_{(cyto,R543A,R616Q)}$) reduced its activity down to the baseline activity level of the R543A mutant (Figure S4J). Thus the R543A mutant does not exhibit concentration dependent activation in the absence of the substrate and also does not require the R-finger residue for its baseline activity. These data strongly support the idea that the active form of EccC is multimeric, but this state is sparsely populated in the absence of the EsxB substrate. However, the activity of this multimeric form is only manifest in the setting of the permissive R543A mutation. These experiments define a hierarchy of activation where both the effect of the R543A mutation and the multimerization are required for appreciable ATPase activity.

EsxB, but not EsxA or EsxBA, Directly Multimerizes EccC Translocase

To probe the multimeric state of *Tc*$EccC_{(cyto)}$ during active catalysis, we used glutaraldehyde crosslinking to capture higher-order multimers. Crosslinking of *Tc*$EccC_{(cyto,R543A)}$ in the presence of native *Tc*EsxB, or with the *Tc*EsxB-*Tc*$EccC_{(cyto,R543A)}$ fusion, revealed both dimer and higher-order oligomeric states that are strongly correlated with activity (Figure 6A). These oligomers were specific to EccC and did not form with the substrate alone (Figure S5A), or when ATPase was incubated with a signal sequence mutant, *Tc*$EsxB_{(V98A)}$ (Figure S5C and S5D). Importantly, while *Tc*EsxB binding was insufficient to activate ATPase activity of the wild-type enzyme (Figure 6A), it effectively drove *Tc*$EccC_{(cyto)}$ into higher-order complexes (Figure S5B and S5D), indicating that substrate-mediated multimerization is not sufficient to override autoinhibition mediated by $ATPase_2$. We found that EsxB exists as a homodimer in isolation (Figure S5E), and thus the substrate

likely stabilizes multimers by first forming EccC:EsxB:EsxB:EccC complexes. Although the addition of EsxB leads to a clear increase in multimerization of the ATPase, it appears to stabilize a state that occurs in the absence of EsxB, as both crosslinking (Figure S5B) and analytical ultracentrifugation (Figure S4F) experiments revealed a low level of EccC multimerization without EsxB.

Surprisingly, addition of *Tc*EsxA, another substrate that forms a tight 1:1 complex with *Tc*EsxB (Figure 2D; Figure S5F, (Renshaw et al., 2002)), but does not directly bind to EccC (Figure S1B and S5G), strongly inhibited ATPase activity in a cooperative manner (Hill coefficient > 2, Figure 6C), suggesting that each *Tc*EsxA molecule affects the activity of more than two *Tc*EccC$_{(cyto,R543A)}$-*Tc*EsxB molecules. The higher-order multimer concentration decreased with increasing *Tc*EsxA in a pattern that directly mirrored the cooperative decrease in ATPase activity (Figure 6C), and this was not affected by mutation of the arginine finger residue (Figure S5H and S5I). Furthermore, addition of *Tc*EsxA to the *Tc*EccC$_{(cyto)}$-*Tc*EsxB chimera led to loss of dimerization of this construct (Figure S5J). Thus, while EsxB homodimers promote assembly and activation of EccC, EsxA binding to EsxB-bound EccC leads to cooperative disassembly and inhibition of the multimeric ATPase.

To test whether EsxA-induced inhibition was due to disruption of the EsxB:EsxB dimerization event, we measured inhibition of ATPase activity in the *Tc*EsxB-*Tc*EccC$_{(cyto,R543A)}$ chimera with increasing concentrations of the signal sequence mutant *Tc*EsxB$_{(V98A)}$, which can still form homodimers but cannot bind to EccC. We found that *Tc*EsxB$_{(V98A)}$ also inhibits activity (Figure S5K), supporting the notion that EsxA inactivates EccC by removing the stabilizing effect of the EsxB:EsxB interaction, presumably by forming EccC:EsxB:EsxA trimers instead of EccC:EsxB:EsxB:EccC tetramers.

Discussion

In this work we have developed a thermophilic model system that allowed for the detailed dissection of the only two components of T7S conserved in all Gram-positive bacteria: EccC and EsxB. Based on our findings we posit a model in which secretory substrates play an active regulatory role in T7S by modulating the activity of EccC (Figure 7). In the absence of EsxB, EccC is monomeric and tightly inactivated via interactions between ATPase$_1$ and ATPase$_2$. EsxB binding to ATPase$_3$, which is relatively weak (~10 μM), drives EccC multimerization, but is not sufficient for activation. Allosteric interactions through displacement of linker$_2$ from pocket$_1$, which relieves the inhibitory interaction with ATPase$_2$, are also required to permit activation of EccC. While we do not yet know the nature of these activation signals, given the linker-pocket architecture found in each ATPase domain we suspect that other substrates and/or T7S components bind to these pockets to create an “AND” logic gate by which secretion of multiple substrates is coordinated, explaining the phenomenon of mutually dependent Type VII secretion (Fortune et al., 2005). The DUF and the transmembrane domains also play an important role in secretion and full delineation of their contribution to the process awaits further experimentation.

This model suggests that T7S activity may be governed by a simple, “just-intime” post-translational control mechanism in which energy is expended only when key substrates are recognized by EccC (Bozdech et al., 2003). T7S may be poised for secretion under all conditions, with EccC waiting for delivery of complete sets of substrates, which would explain why removal of one substrate would inhibit secretion of others. In this way, T7S may not be directly regulated by environmental stimuli, but actuated by signal transduction pathways that regulate synthesis of substrates, such as PhoP/R (Ryndak et al., 2008) and EspR (Raghavan et al., 2008). Although other control mechanisms may be in play, this mode of regulation would not only conserve ATP consumption until it is needed, but would also allow for coordinate secretion of multiple substrates, a function that may be beneficial for the organism.

Our results also suggest that EsxB homodimers, in addition to EsxAB heterodimers (Renshaw et al., 2002), play an important role in Type VII secretion, a notion supported by the observation that ancestral T7S systems, such as those found in the phylum firmicutes, lack EsxA homologs and EsxB exists solely as a homodimer (Poulsen et al., 2014). Experimental evidence from the literature also supports the idea that EsxB dimers have an important physiological role. For example, recent work shows that EsxB in *Bacillus subtilis* is secreted as a dimer (Sysoeva et al., 2014). Likewise, at least four unique crystal structures of different EsxB homodimers from various bacterial species have been deposited in the Protein Data Bank including 2VRZ (Sundaramoorthy et al., 2008), 3GVM (Poulsen et al., 2014), 3ZBH (unpublished) and 3O9O (unpublished). Taken together, we believe that these results provide compelling evidence for the role of EsxB homodimers *in vivo*, and support a model that one role of EsxA is to antagonize the stimulatory effects of EsxB on EccC. How substrates are actually translocated out of the cell upon binding EccC, the oligomeric state of substrates during translocation, and how EccC and/or other T7S proteins modify substrates before export remain important questions that require further study.

Most motor proteins only display maximal ATPase activity in the presence of a mechanical load. Indeed, the activity of EccC, even when activated by the substrate and the R543A mutation, is relatively low. We believe the activity we measure likely represents a basal ATPase rate without the “load” of substrates to be translocated across a membrane. A graded activation of ATPase function is reminiscent of the activation of SecA translocase. In this case, SecA is nearly inactive when cytosolic (Lill et al., 1990), but is partially activated by its interaction with SecYEG, which releases an interdomain, allosteric inhibition in SecA leading to an increase in ATPase activity (Karamanou et al., 2007). The motor is thus primed for the translocation reaction, which is stimulated by its interaction with the signal sequence bearing protein (Chatzi et al., 2014).

Our structural analysis shows other intriguing similarities to the Sec translocation system. The Sec translocase binds to a similar, small helical peptide using mixed electrostatic and hydrophobic interactions. In both cases, the binding occurs in a specialized groove that is distant from the ATPase active site (Gelis et al., 2007) suggesting a role in targeting and orientation of substrates. There are also similarities to targeting of substrates in other secretion systems. For example, in the Type III secretion system a targeting sequence on a chaperone protein, CesAB, is required for interaction with the Type III ATPase, however the

actual translocation is mediated by an entirely different signal (Chen et al., 2013). Given that several other regions of the EsxB and EsxA proteins have been implicated in translocation (Daleke et al., 2012; Sysoeva et al., 2014) we suspect a similar division between targeting and substrate orientation is also present in the Type VII system.

The EccC ATPase is phylogenetically related to the T4 secretion system coupling proteins, typified by the VirD4 ATPase in *Agrobacterium tumefaciens* (Guglielmini et al., 2013). These proteins also bind to a C-terminal sequence on substrate proteins that is necessary for secretion but the molecular interactions and biochemical effects of substrate binding in these systems is unknown (Trokter et al., 2014). In the *A. tumefaciens* system, three monomeric ATPases (VirB4, VirD4 and VirB11) are required for secretion of substrates by the system. It is intriguing to speculate that these three ATPases, which all appear to serve very different mechanistic purposes, may carry out functions analogous to the three ATPase domains of EccC, but this hypothesis awaits further structural information about the assembly and function of EccC and of the T4 secretion ATPases.

Targeting T7S for inhibition is an attractive antibacterial strategy, given the centrality of these systems to pathogenesis in *M. tuberculosis* and *S. aureus*, and their wide distribution among gram-positive bacteria (Chen et al., 2010). Our work suggests two unexpected targets for disruption of the function of T7 secretion. First, small molecules targeted to the inactive state of $ATPase_1$ may stabilize its autoinhibition (Schindler et al., 2000). Secondly, the interaction pocket for the substrate is quite deep and may be amenable to small molecule targeting. Additionally, knowing the molecular determinants of signal sequence recognition may also allow us to design improved vaccine strains, which export subsets of immunodominant virulence factors but do not cause disease.

Experimental Procedures

A full description of the methods, reagents and crystallographic statistics is included in the supplemental materials.

Mycobacterial mutants and secretion assays

The Δ*eccCa*$_{1Mt}$-Δ*eccCb*$_{1Mt}$ deletion strain was created by homologous recombination using specialized transducing phage as previously described (Glickman et al., 2000). Complementation of the *eccC* null mutant was carried out by cloning the entire *M. tuberculosis rv3870-rv3871* locus into an integrating vector containing a C- terminal flag tag and under the control of the predicted native promoter. Secretion assays were performed as described previously (Ohol et al., 2010).

Protein expression and purification

Recombinant proteins were subcloned by PCR into a pET vector system and expressed and purified from C41(DE3) strain *E. coli* using standard techniques. Details are available in the Supplemental Experimental Procedures.

Electron microscopy

Single particles were picked from uranyl acetate-stained images and processed into classes containing approximately 60 images. Reconstructions were accomplished as described in the Supplemental Experimental Procedures.

Crystallization and structure solution

Crystallization and structure solution are described in detail in the Supplemental Experimental Procedures. For the $EccC_{Tc(\ 199\text{-}1315)}$ structure, initial phases were determined with SAD phasing of a Ta_6Br_{12} derivative at ~7.5 Å, then improved by MIR phasing with Pt and Hg derivatives. An anomalous difference map determined by comparison to a selenomethionine derivative assisted model building. The other structures were solved using standard methods.

Biochemical assays

Steady-state ATPase activity was analyzed using an assay that continuous coupled assay (Kornberg and Pricer, 1951) adapted to a 96 well format.

Fluorescence aniostropy was performed using a 5-FAM-VNRVQALLNG peptide interacting with the $EccC_{Tc(\ 199\text{-}1315)}$ construct as described in the Supplemental Experimental Methods.

For crosslinking assays, 2-5 μg of total protein was incubated with 0.2% glutaraldehyde for 10 minutes and then quenched with 1 M Tris pH 8.0. Denaturing gels were stained with Coomassie or western blotted. A full description is available in the Supplemental Experimental Methods.

Bioinformatics

We attempted to identify all P-loop ATPases in the PDB on a per chain basis and then analyzed the position of the Walker A lysine side chain relative to the position of the Walker B aspartic acid using programs designed by the authors. The initial list and the sorted lists described in the text are available in Supplemental Table 4. Please see the Supplemental Experimental Methods for full details.

Genetic interaction studies

Directed yeast-two-hybrid studies were performed using a LacZ reporter system as described previously (Champion et al., 2006). Strain names and additional procedures are available in the Supplementary Experimental Procedures.

Supplementary Material

Refer to Web version on PubMed Central for supplementary material.

Acknowledgments

We acknowledge support from the NIH (K08AI091656 to OSR, R01AI081727 to JSC and U54GM094625 to RMS) and the NSF (Grant No. 1144247 to DD).

For technical assistance we thank Rebecca Robbins, Peter Bieling, Jenifer Du Mond, Lara Koehler, R. Stefan Isaac, Yaneth Robles, Diana Romero, Spenser Alexander and Andrew Rodriguez. For helpful discussions we thank Ron Vale, John Kuriyan, James Berger, Bennett Penn, Matt Lohse and Damian Ekiert.

We thank R. Rajashankar at the APS beamline NE-CAT 24ID, George Meigs and Jane Tanamachi at ALS BL 8.3.1 and Tzanko Doukov and Lisa Dunn at SSRL. APS is supported by the U.S. DOE Contract DE-AC02-06CH11357. ALS is supported by the U.S. DOE Contract DE-AC02-05CH11231. The SSRL Structural Molecular Biology Program is supported by the U.S. DOE Office of Biological and Environmental Research, and by the NIH-GMS, (including P41GM103393).

References

Abdallah AM, Gey van Pittius NC, Champion PAD, Cox J, Luirink J, Vanden-broucke-Grauls CMJE, Appelmelk BJ, Bitter W. Type VII secretion--mycobacteria show the way. Nat Rev Microbiol. 2007; 5:883–891. [PubMed: 17922044]

Ahmadian MR, Stege P, Scheffzek K, Wittinghofer A. Confirmation of the arginine-finger hypothesis for the GAP-stimulated hydrolysis reaction of Ras. Nat Struct Mol Biol. 1997; 4:686–689.

Berman HM, Battistuz T, Bhat TN, Bluhm WF, Bourne PE, Burkhardt K, Feng Z, Gilliland GL, Iype L, Jain S, et al. The Protein Data Bank. Acta Crystal-logr D Biol Crystallogr. 2002; 58:899–907.

Besprozvannaya M, Pivorunas VL, Feldman Z, Burton BM. SpoIIIE achieves directional DNA translocation through allosteric regulation of ATPase activity by an accessory domain. J Biol Chem. 2013

Bitter W, Houben ENG, Bottai D, Brodin P, Brown EJ, Cox JS, Derbyshire K, Fortune SM, Gao L-Y, Liu J, et al. Systematic genetic nomenclature for type VII secretion systems. PLoS Pathog. 2009; 5:e1000507. [PubMed: 19876390]

Bozdech Z, Llinás M, Pulliam BL, Wong ED, Zhu J, DeRisi JL. The transcriptome of the intraerythrocytic developmental cycle of Plasmodium falciparum. PLoS Biol. 2003; 1:E5. [PubMed: 12929205]

Brodin P, Majlessi L, Marsollier L, de Jonge MI, Bottai D, Demangel C, Hinds J, Neyrolles O, Butcher PD, Leclerc C, et al. Dissection of ESAT-6 system 1 of Mycobacterium tuberculosis and impact on immunogenicity and virulence. Infect Immun. 2006; 74:88–98. [PubMed: 16368961]

Burts ML, Williams WA, DeBord K, Missiakas DM. EsxA and EsxB are secreted by an ESAT-6-like system that is required for the pathogenesis of Staphylococcus aureus infections. Proc Natl Acad Sci USa. 2005; 102:1169–1174. [PubMed: 15657139]

Carter AP, Cho C, Jin L, Vale RD. Crystal structure of the dynein motor domain. Science. 2011; 331:1159–1165. [PubMed: 21330489]

Champion PAD, Stanley SA, Champion MM, Brown EJ, Cox JS. C-terminal signal sequence promotes virulence factor secretion in Mycobacterium tuberculosis. Science. 2006; 313:1632–1636. [PubMed: 16973880]

Chatzi KE, Sardis MF, Economou A, Karamanou S. SecA-mediated targeting and translocation of secretory proteins. Biochim Biophys Acta. 2014; 1843:1466–1474. [PubMed: 24583121]

Chen JM, Pojer F, Blasco B, Cole ST. Towards anti-virulence drugs targeting ESX-1 mediated pathogenesis of Mycobacterium tuberculosis. Drug Discovery Today: Disease Mechanisms. 2010; 7:e25–e31.

Chen L, Ai X, Portaliou AG, Minetti CASA, Remeta DP, Economou A, Kalodimos CG. Substrate-Activated Conformational Switch on Chaperones Encodes a Targeting Signal in Type III Secretion. Celrep. 2013; 3:709–715.

Daleke, MH.; Ummels, R.; Bawono, P.; Heringa, J.; Vandenbroucke-Grauls, CMJE.; Luirink, J.; Bitter, W. General secretion signal for the mycobacterial type VII secretion pathway. 2012.

Davis JM, Ramakrishnan L. The role of the granuloma in expansion and dissemination of early tuberculous infection. Cell. 2009; 136:37–49. [PubMed: 19135887]

Erzberger JP, Berger JM. Evolutionary relationships and structural mechanisms of AAA+ proteins. Annu Rev Biophys Biomol Struct. 2006; 35:93–114. [PubMed: 16689629]

Fortune SM, Jaeger A, Sarracino DA, Chase MR, Sassetti CM, Sherman DR, Bloom BR, Rubin EJ. Mutually dependent secretion of proteins required for mycobacterial virulence. Proc Natl Acad Sci USa. 2005; 102:10676–10681. [PubMed: 16030141]

Gao L-Y, Guo S, McLaughlin B, Morisaki H, Engel JN, Brown EJ. A mycobacterial virulence gene cluster extending RD1 is required for cytolysis, bacterial spreading and ESAT-6 secretion. Mol Microbiol. 2004; 53:1677–1693. [PubMed: 15341647]

Gelis I, Bonvin AMJJ, Keramisanou D, Koukaki M, Gouridis G, Karamanou S, Economou A, Kalodimos CG. Structural basis for signal-sequence recognition by the translocase motor SecA as determined by NMR. Cell. 2007; 131:756–769. [PubMed: 18022369]

Gomis-Rüth FX, Moncalián G, Pérez-Luque R, González A, Cabezón E, de la Cruz F, Coll M. The bacterial conjugation protein TrwB resembles ring hel-icases and F1-ATPase. Nature. 2001; 409:637–641. [PubMed: 11214325]

Guglielmini J, de la Cruz F, Rocha EPC. Evolution of Conjugation and Type IV Secretion Systems. Molecular Biology and Evolution. 2013; 30:315–331. [PubMed: 22977114]

Guinn KM, Hickey MJ, Mathur SK, Zakel KL, Grotzke JE, Lewinsohn DM, Smith S, Sherman DR. Individual RD1-region genes are required for export of ESAT-6/CFP-10 and for virulence of Mycobacterium tuberculosis. Mol Microbiol. 2004; 51:359–370. [PubMed: 14756778]

Houben ENG, Korotkov KV, Bitter W. Take five - Type VII secretion systems of Mycobacteria. Biochim Biophys Acta. 2014; 1843:1707–1716. [PubMed: 24263244]

Hsu T, Hingley-Wilson SM, Chen B, Chen M, Dai AZ, Morin PM, Marks CB, Padiyar J, Goulding C, Gingery M, et al. The primary mechanism of attenuation of bacillus Calmette-Guerin is a loss of secreted lytic function required for invasion of lung interstitial tissue. Proc Natl Acad Sci USa. 2003; 100:12420–12425. [PubMed: 14557547]

Huppert LA, Ramsdell TL, Chase MR, Sarracino DA, Fortune SM, Burton BM. The ESX System in Bacillus subtilis Mediates Protein Secretion. PLoS ONE. 2014; 9:e96267. [PubMed: 24798022]

Karamanou S, Vrontou E, Sianidis G, Baud C, Roos T, Kuhn A, Politou AS, Economou A. A molecular switch in SecA protein couples ATP hydrolysis to protein translocation. Mol Microbiol. 1999; 34:1133–1145. [PubMed: 10594836]

Karamanou S, Gouridis G, Papanikou E, Sianidis G, Gelis I, Keramisanou D, Vrontou E, Kalodimos CG, Economou A. Preprotein-controlled catalysis in the helicase motor of SecA. Embo J. 2007; 26:2904–2914. [PubMed: 17525736]

Kornberg A, Pricer WE. Enzymatic phosphorylation of adenosine and 2,6-diaminopurine riboside. J Biol Chem. 1951; 193:481–495. [PubMed: 14907737]

Lill R, Dowhan W, Wickner W. The ATPase activity of SecA is regulated by acidic phospholipids, SecY, and the leader and mature domains of precursor proteins. Cell. 1990; 60:271–280. [PubMed: 2153463]

Mahairas GG, Sabo PJ, Hickey MJ, Singh DC, Stover CK. Molecular analysis of genetic differences between Mycobacterium bovis BCG and virulent M. bovis J Bacteriol. 1996; 178:1274–1282.

Massey TH, Mercogliano CP, Yates J, Sherratt DJ, Löwe J. Double-stranded DNA translocation: structure and mechanism of hexameric FtsK. Mol Cell. 2006; 23:457–469. [PubMed: 16916635]

Menz RI, Walker JE, Leslie AG. Structure of bovine mitochondrial F(1)-ATPase with nucleotide bound to all three catalytic sites: implications for the mechanism of rotary catalysis. Cell. 2001; 106:331–341. [PubMed: 11509182]

Ohol YM, Goetz DH, Chan K, Shiloh MU, Craik CS, Cox JS. My-cobacterium tuberculosis MycP1 protease plays a dual role in regulation of ESX-1 secretion and virulence. Cell Host Microbe. 2010; 7:210–220. [PubMed: 20227664]

Pallen MJ. The ESAT-6/WXG100 superfamily -- and a new Gram-positive secretion system? Trends Microbiol. 2002; 10:209–212. [PubMed: 11973144]

Peña A, Ripoll-Rozada J, Zunzunegui S, Cabezón E, la Cruz de F, Arechaga I. Autoinhibitory regulation of TrwK, an essential VirB4 ATPase in type IV secretion systems. J Biol Chem. 2011; 286:17376–17382. [PubMed: 21454654]

Poulsen C, Panjikar S, Holton SJ, Wilmanns M, Song YH. WXG100 Protein Superfamily Consists of Three Subfamilies and Exhibits an α-Helical C-Terminal Conserved Residue Pattern. PLoS ONE. 2014; 9:e89313. [PubMed: 24586681]

Pym AS, Brodin P, Majlessi L, Brosch R, Demangel C, Williams A, Griffiths KE, Marchal G, Leclerc C, Cole ST. Recombinant BCG exporting ESAT-6 confers enhanced protection against tuberculosis. Nat Med. 2003; 9:533–539. [PubMed: 12692540]

Raghavan S, Manzanillo P, Chan K, Dovey C, Cox JS. Secreted transcription factor controls Mycobacterium tuberculosis virulence. Nature. 2008; 454:717–721. [PubMed: 18685700]

Ramsdell TL, Huppert LA, Sysoeva TA, Fortune SM, Burton BM. Linked Domain Architectures Allow for Specialization of Function in the FtsK/SpoIIIE ATPases of ESX Secretion Systems. J Mol Biol. 2014

Renshaw PS, Lightbody KL, Veverka V, Muskett FW, Kelly G, Frenkiel TA, Gordon SV, Hewinson RG, Burke B, Norman J, et al. Structure and function of the complex formed by the tuberculosis virulence factors CFP-10 and ESAT-6. Embo J. 2005; 24:2491–2498. [PubMed: 15973432]

Renshaw PS, Panagiotidou P, Whelan A, Gordon SV, Hewinson RG, William-son RA, Carr MD. Conclusive evidence that the major T-cell antigens of the Mycobacterium tuberculosis complex ESAT-6 and CFP-10 form a tight, 1:1 complex and characterization of the structural properties of ESAT-6, CFP-10, and the ESAT-6*CFP-10 complex. Implications for pathogenesis and virulence. J Biol Chem. 2002; 277:21598–21603. [PubMed: 11940590]

Ryndak M, Wang S, Smith I. PhoP, a key player in Mycobacterium tuberculosis virulence. Trends Microbiol. 2008; 16:528–534. [PubMed: 18835713]

Schindler T, Bornmann W, Pellicena P, Miller WT, Clarkson B, Kuriyan J. Structural mechanism for STI-571 inhibition of abelson tyrosine kinase. Science. 2000; 289:1938–1942. [PubMed: 10988075]

Senior AE. Two ATPases. J Biol Chem. 2012; 287:30049–30062. [PubMed: 22822068]

Stanley SA, Raghavan S, Hwang WW, Cox JS. Acute infection and macrophage subversion by Mycobacterium tuberculosis require a specialized secretion system. Proc Natl Acad Sci USa. 2003; 100:13001–13006. [PubMed: 14557536]

Sundaramoorthy R, Fyfe PK, Hunter WN. Structure of Staphylococcus aureus EsxA suggests a contribution to virulence by action as a transport chaperone and/or adaptor protein. J Mol Biol. 2008; 383:603–614. [PubMed: 18773907]

Sysoeva TA, Zepeda-Rivera MA, Huppert LA, Burton BM. Dimer recognition and secretion by the ESX secretion system in Bacillus subtilis. Proc Natl Acad Sci USa. 2014

Trokter M, Felisberto-Rodrigues C, Christie PJ, Waksman G. ScienceDirectRecent advances in the structural and molecular biology of type IV secretion systems. Curr Opin Struct Biol. 2014; 27:16–23. [PubMed: 24709394]

Waksman G. Bacterial secretion comes of age. Philos Trans R Soc Lond, B, Biol Sci. 2012; 367:1014–1015. [PubMed: 22411974]

Walker JE. The ATP synthase: the understood, the uncertain and the unknown. Biochem Soc Trans. 2013; 41:1–16. [PubMed: 23356252]

Wendler P, Ciniawsky S, Kock M, Kube S. Structure and function of the AAA+ nucleotide binding pocket. Biochim Biophys Acta. 2012; 1823:2–14. [PubMed: 21839118]

Highlights

- X-ray and EM structures reveal the structure the Type VII secretion ATPase EccC
- EccC is a unique, linear array of three interlocking ATPase domains
- The secretion substrate EsxB binds to an unexpected pocket on the third ATPase domain
- Binding of substrates controls multimerization and activation of EccC

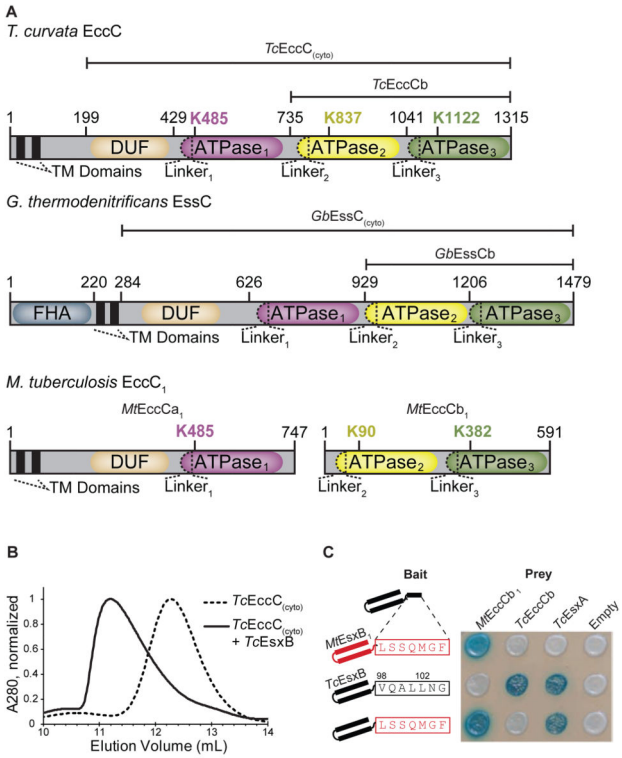

Figure 1. The EccC ATPase has a unique, conserved domain structure and binds to the EsxB signal sequence

(A) Domain structure of the EccC and EssC ATPases. **(B)** Size exclusion chromatography showing that *Tc*EsxB binds to *Tc*EccC$_{(cyto)}$ and induces a large shift in elution volume. **(C)** Yeast-two-hybrid analysis of interactions between EccC and EsxB. Wild-type *Tc*EsxB and *Mt*EsxB$_1$ are directed specifically to their cognate ATPase via the last seven amino acids (boxed), which are not required for interaction with EsxA. Also see Figure S1

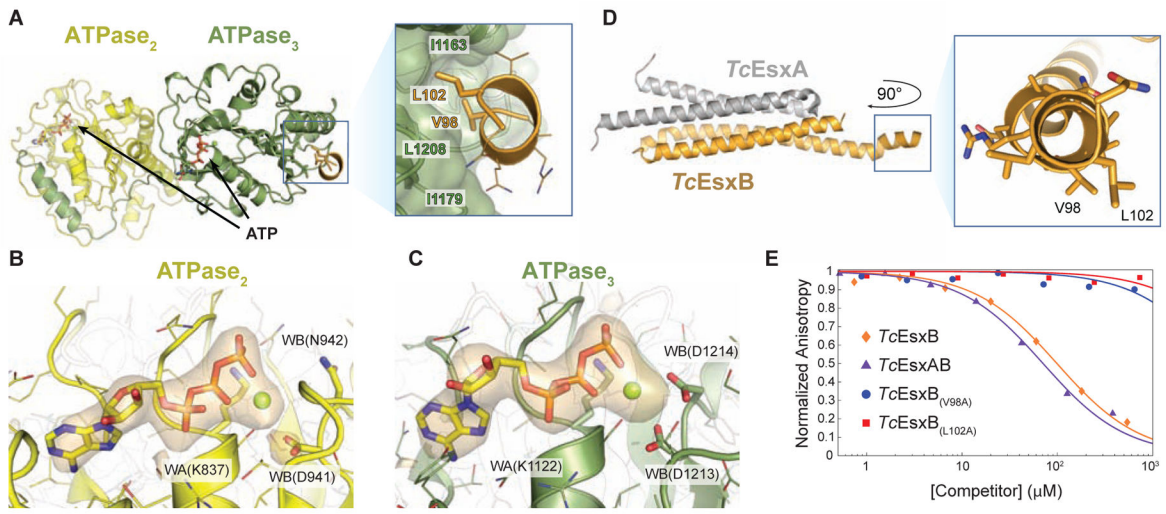

Figure 2. Co-crystal structure reveals signal sequence binding pocket in *Tc*EccCb

(A) The crystal structure of *Tc*EccCb (ATPase domains colored as in Figure 1A) bound to the C-terminal signal sequence of *Tc*EsxB (gold). Binding of the C-terminal amino acids of *Tc*EsxB to $ATPase_3$ is mediated by interactions with two conserved hydrophobic residues that bind in a hydrophobic binding pocket. Only the C-terminal signal sequence residues are interpretable in the electron density (Figure S2A), and the Y-X-X-X-D/E motif implicated in secretion (Daleke et al., 2012) appears disordered in the crystal. **(B–C)** The orange volume represents the simulated-annealing difference-density map calculated for $ATPase_2$ **(B)** and $ATPase_3$ **(C)** without nucleotide and contoured at 4 σ. **(D)** X-ray structure of *Tc* the EsxAB heterodimer with a close-up view of the C-terminal signal sequence helix. V98 and L102, which are necessary for binding to *Tc*EccC, are labeled. **(E)** Binding of a fluorescently labeled signal sequence peptide (5-FAM-VNRVQALLNG) to $TcEccC_{(cyto)}$ monitored in the presence of increasing concentrations of unlabeled competing full length *Tc*EsxB. Wild-type *Tc*EsxB and *Tc*EsxAB heterodimer compete with the peptide. Mutations in L102 or V98 prevent competition with the wild-type peptide, indicating that they do not bind. Presented data are representative experiments. Also see Figure S2.

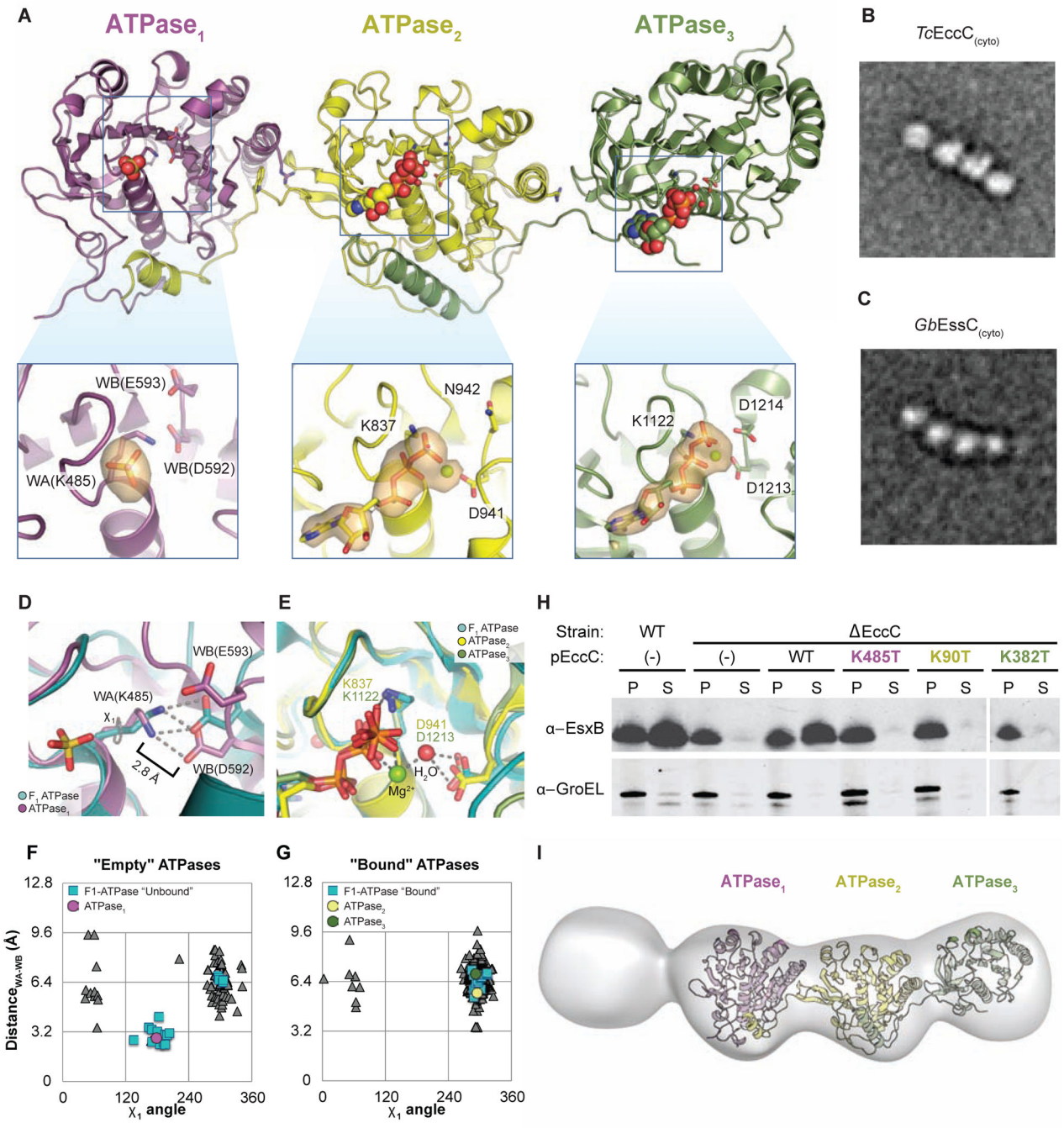

Figure 3. ATPase$_1$ is autoinhibited and integrated into a ridged array of ATPase domains

(A) The crystal structure of *Tc*EccC$_{(cyto)}$ highlighting the differences between the ATP-bound catalytic sites of ATPase$_2$ and ATPase$_3$ and the nucleotide free site of ATPase$_1$. The orange volume represents a simulated-annealing difference-density map calculated without nucleotide or sulfate and contoured at 3 σ. Note that the ATPase$_3$ insert has been rotated slightly to allow for comparison between the ATPase active sites **(B–C)** Representative EM class average of **(B)** *Tc*EccC$_{(cyto)}$ and (*Gb***C)** EssC$_{(cyto)}$ showing the linear structure of EccC. Scale bars are 100 Å. **(D)** ATPase$_1$ (purple), with the "empty" subunit of F$_1$-ATPase

(PDB 1H8H) overlaid in cyan and **(E)** $ATPase_2$ (yellow) and $ATPase_3$ (green) overlaid with the AMP-PNP-bound subunit of F_1-ATPase (cyan) from 1H8H. **(F)** A graph representing the distance between the Walker A lysine amino group and the closest Walker B carboxylate oxygen, as a function of the rotameric position of the Walker A lysine. Each triangle represents one of 311 pdb chains of an ATP bound, P-loop ATPase identified by our protocol (see supplementary methods). **(G)** A similar graph to **(F)** except the triangle represents the residues of "empty" ATPases from PDB entries that contain both a bound and unbound P-loop ATPase domain in the same file. **(H)** Western blot detection of *Mt*$EsxB_1$ and GroEL from cell supernatants (S) and cell pellet lysate (P) fractions of *Mt*$EccC_1$ knockout and complemented cells. **(I)** Three- dimensional reconstruction at an estimated resolution of 23 Å, based on 1634 images in the presence of 1 mM ATP-γS and 10 mM $MgCl_2$. The model has been contoured to fit the crystal structure. Though it is impossible to resolve the difference between the first and fourth domains, the electron density of one is much lower than the other three, suggesting this domain is the DUF domain, which is disordered in the crystal structure. Also see Figure S3.

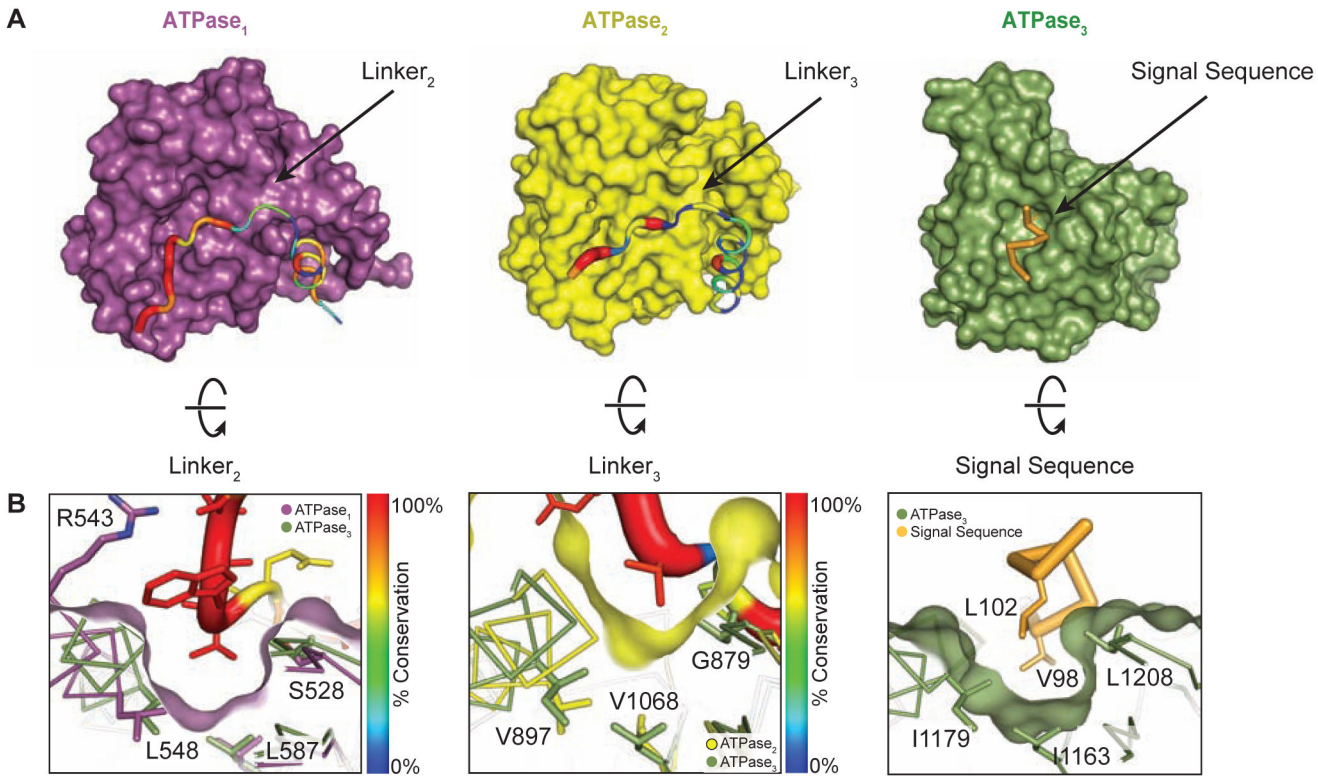

Figure 4. Residues in linker$_2$ and linker$_3$ mimic the substrate and bind to pocket$_1$ and pocket$_2$ on *Tc*EccC

(A) The individual ATPase domains are shown and have been rotated to reveal the path of the linker across the ATPase domain. The linker is colored and weighted in diameter according to the degree of conservation across 142 unique EccC sequences. **(B)** The surface has been rotated to highlight the linker groove. ATPase$_3$ and the pocket residues (Figure S2C) overlay ATPase$_1$ and ATPase$_2$ to highlight the homologies in the linker binding and signal sequence binding pockets. The ATPase$_2$ pocket is significantly shallower than ATPase$_1$ and ATPase$_3$.

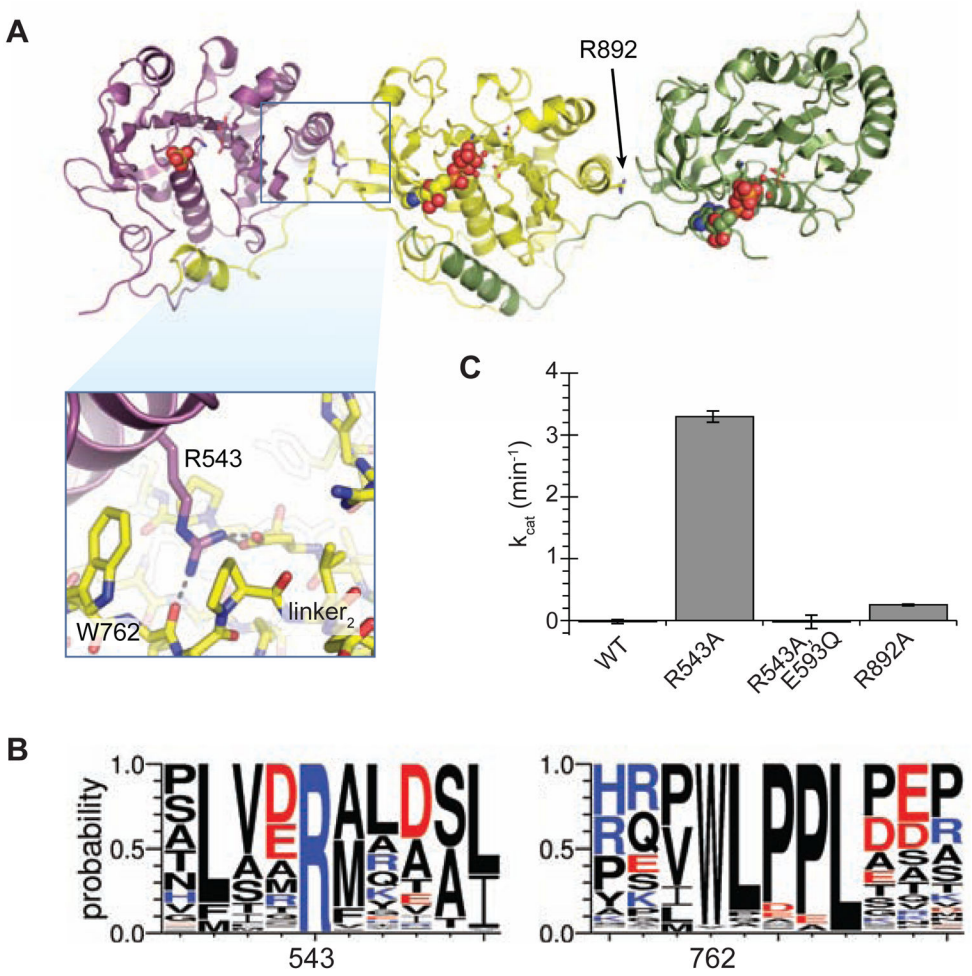

Figure 5. ATPase$_1$ is held in an autoinhibited state by inter-ATPase interactions

(A) Crystal structure of *Tc*EccC$_{(cyto)}$ with inset highlighting the interface between ATPase$_1$ and ATPase$_2$. **(B)** Logo diagram representing the alignment of 142 unique EccC sequences. **(C)** Disruption of ATPase$_1$-ATPase$_2$ interface by R543A mutation activates the ATPase activity of *Tc*EccC, which requires the Walker B catalytic residue in ATPase$_1$ (E593Q). An analogous mutation between ATPase$_2$ and ATPase$_3$, R892A, led to a small increase in activity. The graph represents three measurements of ATPase activity at an enzyme concentration of 1 μM ATPase with saturating ATP*$MgCl_2$ (10 mM). Also see Figure S4.

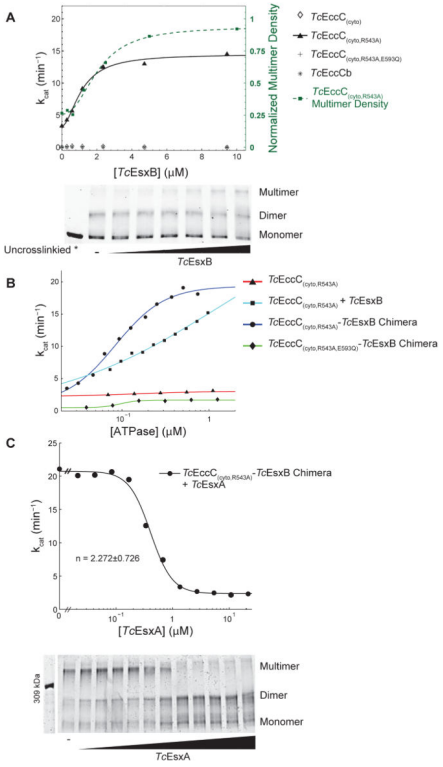

Figure 6. EsxB and EsxA substrates control EccC activity via regulating enzyme multimerization

(A) The ATPase activity of the indicated *Tc*EccC proteins was measured at different concentrations of *Tc*EsxB. Multimerization of *Tc*EccC$_{(cyto,R543A)}$, detected by glutaraldehyde crosslinking (bottom panel), increases with addition of *Tc*EsxB (0–10 μM). Quantification of the multimer band is also indicated on the ATPase activity graph (green dotted line with squares) to demonstrate correlation between multimer concentration and activity. (**B**) ATPase activity of the indicated proteins, either *Tc*EccC$_{(cyto,R543A)}$ +/− *Tc*E*Tc*sxB EccC or $_{(cyto,R543A)}$-*Tc*EsxB chimeras, was measured as a function of enzyme concentration. In **(B)** and **(C)** each point represents the mean of three independent measurements. **(C)** ATPase activity of the *Tc*EccC$_{(cyto,R543A)}$-*Tc*EsxB chimera was measured at different concentrations of *Tc*EsxA (top panel), and multimerization of the enzyme in these reactions was assessed by glutaraldehyde crosslinking followed by SDS-PAGE (bottom panel - top concentration of *Tc*EsxA is 22 μM and concentrations are reduced 2-fold in each lane to the left). See also Figure S5.

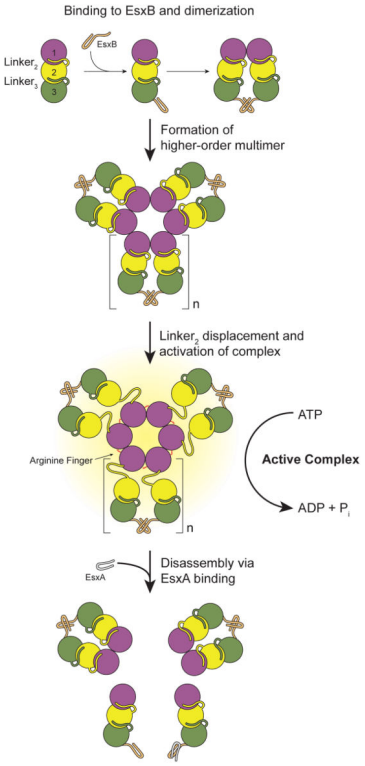

Figure 7. Model of substrate-mediated activation of EccC

In the absence of substrates EccC is monomeric. Interaction with EsxB leads to dimerization of the ATPase and then higher order multimerization, but cannot activate the enzyme. In this study we used the R543A mutation to disrupt the interaction between $ATPase_1$ and $ATPase_2$ although *in vivo* this role may be played by other proteins that bind to $ATPase_1$ analogously to the binding of EsxB to $ATPase_3$, or other signals. Once $ATPase_1$ is displaced, EccC is activated further by multimerization mediated by a conserved R-finger. EsxA can disrupt the EsxB:EsxB interaction and disassemble the multimer. We have no evidence for the structure of the EccC:EsxB dimer or stiochiomtry and structure of the multimeric form. Thus, both these aspects of the model are speculative, though based on prior structures of related substrate proteins (i.e. 3GVM) and the FtsK-like ATPases (i.e. 2IUU). We have indicated this ambiguity with the variable “n” for the number of subunits in the multimer.